ELSEVIER

Tectonophysics 329 (2000) 39–60

TECTONOPHYSICS

www.elsevier.com/locate/tecto

Effective elastic thickness of the northern Australian continental lithosphere subducting beneath the Banda orogen (Indonesia): inelastic failure at the start of continental subduction

K. Tandon[a,*], J.M. Lorenzo[a], G.W. O'Brien[b]

[a]*Department of Geology and Geophysics, Louisiana State University, Baton Rouge, LA 70803, USA*
[b]*Australian Geological Survey Organization, G.P.O. Box 378, Canberra 2601, Australia*

Received 1 February 1999; accepted 17 November 1999

Abstract

Pliocene-Recent continent-island arc collision of the northern Australian continental lithosphere across the Banda orogen from Roti to the Kai Plateau (~121–137°E longitude) has formed an underfilled foreland basin within the Timor–Tanimbar–Aru Trough. Continental collision on northern Australian lithosphere is most advanced near central Timor Island in terms of shortening and absorbing the forearc basin (Savu Basin) within the accretionary prism. Australian continental lithosphere north of area around central Timor Island is believed to be detached from the oceanic lithosphere. Effective Elastic Thickness (EET) of the northern Australian continental lithosphere from Roti to the Kai Plateau are derived using an elastic half-beam model. Modeled deflection is matched to the seafloor bathymetry and the marine complete 3D Bouguer gravity anomalies. The EET varies from 27 to 75 km across the northern Australian continental lithosphere from Roti to Kai Plateau when the thickness of the elastic half-beam is kept constant. The highest EET values lies near central Timor. From the shelf to beneath the Banda orogen, the EET of the northern Australian continental lithosphere is reduced from ~90 to ~30 km when the thickness of the elastic half-beam is allowed to vary down dip. Elastic half-beam modeling approximates the Banda orogen as a triangular load and hidden subsurface loads as end-point loads. Wider triangular loads modeling the load contribution from Banda orogen need higher values of EET. Such an observation highlights the role of high EET in thin-skinned collisional tectonics by promoting the support of wider accretionary prisms by parts of foreland basins with higher EET. Variations in EET may result from inelastic yielding in the northern Australian continental lithosphere. Oroclinal bending of the Australian continental lithosphere in the east, from Tanimbar to the Kai Plateau, may create additional yielding and further decrease the EET. Change in EET occurred at the start of continental subduction in the late Miocene–early Pliocene boundary due to change in curvature of the northern Australian lithosphere near the shelf-slope, both in map and cross-sectional view. Evidence for the inelastic yielding of the northern Australian continental lithosphere near the present-day shelf-slope at the continental subduction is found in: (1) the maximum change of EET near shelf-slope in laterally variable EET calculations, and (2) in the almost cessation of normal faulting in late Miocene–early Pliocene seen on seismic reflection data from northern Australian continental shelf-slope. Elastic half-beam models across central Timor do not require end-point loads and may imply that there are no slab pull forces from the

* Corresponding author. Laboratory for Computational Geodynamics, Department of Chemistry, Indiana University, Bloomington, IN 47405, USA. Tel.: +1-812-855-2047; fax: +1-812-855-8300.

E-mail addresses: ktandon@indiana.edu (K. Tandon), juan@geol.lsu.edu (J.M. Lorenzo), gobrien@selenite.agso.gov.au (G.W. O'Brien).

PII: S0040-1951(00)00187-6

oceanic lithosphere that are acting on the leading edge of the subducted northern Australian continental lithosphere.

Keywords: basin formation; continental collision; flexure; inelastic failure; lithospheric rigidity; Timor–Tanimbar–Aru trough; foreland basins

1. Introduction

Continents can show a wide variation in their Effective Elastic Thickness (EET) within the same orogen as a result of inelastic and/or thermal processes (McNutt et al., 1988; Burov and Diament, 1995, 1996; Stewart and Watts, 1997). EET measures the ability of the lithosphere to support loads regionally rather than respond in a local Airy isostatic manner (zero EET) (Watts, 1983). EET values serve to compare lithospheric flexural rigidity within and between continental collisional regions (McNutt et al., 1988; Stewart and Watts, 1997). Watts et al. (1995) advocate that the highest EET should be found where the collision is maximum in terms of shortening. Pre-collisional high EET facilitates thin-skinned, low-angle fold and thrust tectonics, and back-thrusting on a low-angle flexurally more rigid plate (Watts et al., 1995). Karig et al. (1976) also found that lower slope on the outer trench and lower forebulges, indicative of high EET in oceanic lithosphere, world-wide correlates with wider accretionary prisms.

Change in the EET of the continental lithosphere in a collisional environment can occur for several reasons. One of them is the difference in bending

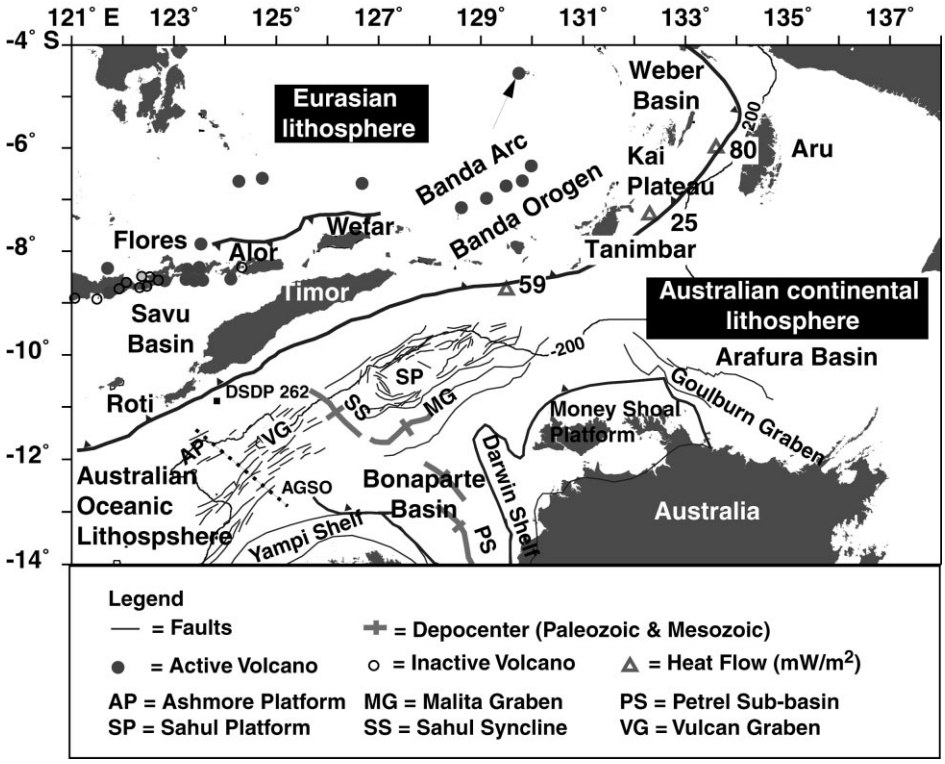

Fig. 1. General tectonic map for the northern Australian continental lithosphere across the Banda Arc (Hamilton, 1974; Veevers et al. 1974; Stagg, 1993; AGSO North West Shelf Study Group, 1994; Snyder et al., 1996). Heat flow values are from Bowin et al. (1980). The thick line with black triangles (point to overthrust plate) shows the subduction boundary between the northern Australian continental lithosphere and the Eurasian lithosphere in Timor–Tanimbar–Aru Trough; north of Alor and Wetar, it denotes the back-thrusting. Thick dashed line lettered "AGSO" marks the location for seismic track of AGSO line 98R08 (Lorenzo et al., 1998). The 200 m bathymetry contour marks the continental shelf-slope boundary from ETOPO-5 (National Geophysical Data Center, 1988).

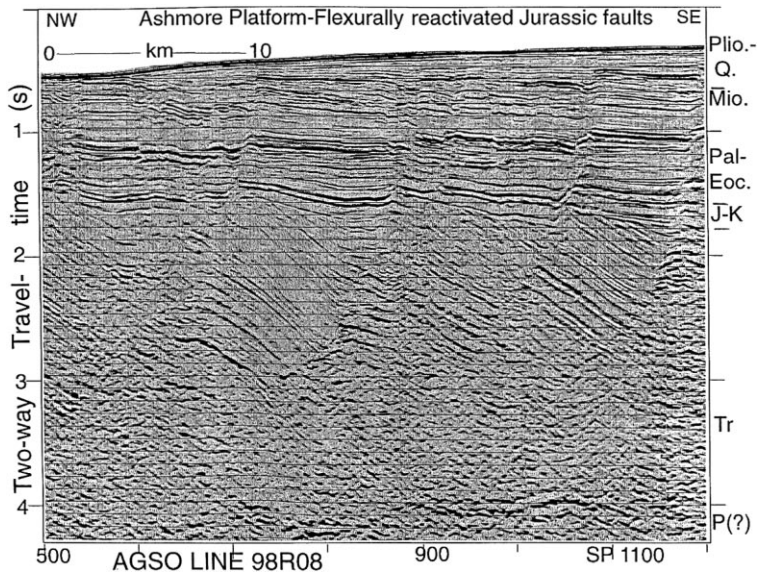

Fig. 2. Uninterpreted migrated seismic reflection AGSO line 98R08 on the northern Australian continental shelf southwest of Timor Island (Lorenzo et al., 1998). Age abbreviations: Plio(cene)-Q(Recent), Mio(cene), J(urassic)-K(Cretaceous), Tr(iassic), and P(ermian). The seismic section shows how the extent of normal faulting changes with time. The location of the seismic line is shown in Fig. 1.

stress within the lithosphere will cause varying degrees of inelastic failure and differences in EET values (McNutt et al., 1988). Inelastic yielding can be caused by: (1) brittle and plastic failure of the lithosphere, (2) brittle–ductile decoupling in the upper-middle crust, and (3) crust–mantle decoupling (McAdoo et al., 1978; McNutt et al., 1988; Burov and Diament, 1995, 1996; Dresen et al., 1997). Decoupling can reduce the EET to that of the thickest competent unit within the lithosphere (Burov and Diament, 1995). Oroclinal bending of the lithosphere can also decrease EET (McNutt et al., 1988).

Inheritance of thermal structure from previous rifting (sub-basins on the shelf of northern Australian continental lithosphere in Fig. 1) may control the distribution of EET (Bertotti et al., 1997; Stewart and Watts, 1997). Thrusting of the sediments could also decrease the EET of the lithosphere beneath by thermally blanketing the crust by low conductivity sediments and increasing the thickness of weaker crust (Kusznir and Karner, 1985; Steckler and ten Brink, 1986; Burov and Diament, 1995 and 1996; Lavier and Steckler, 1997). Changes in EET due to the variations in the thickened sedimentary cover and crustal thickening would only occur in the northern Australian continental lithosphere beneath the Banda orogen.

We perform elastic half-beam modeling to calculate EET from Roti to the Kai Plateau (west of Aru Island) traversing Timor and Tanimbar Islands (~121–137°E longitude) (Fig. 1) by matching the flexure response to seafloor and marine complete 3D Bouguer gravity anomalies. Across the northern Australian continental lithosphere, we make first order EET estimations with an uniform thickness of EET down dip using 15 profiles. However, constant EET does not account for the change in EET from shelf to beneath the orogen. To study the effect of inelastic yielding down dip for the northern Australian continental lithosphere, a profile with laterally variable EET is also calculated. Laterally variable EET calculation attempts to better fit the deflection data.

We attempt to link the calculations for EET to the varying degree of shortening within Banda orogen caused by the collision of northern Australian continental lithosphere. Variations in EET are manifested by the changes in curvature of the northern Australian continental lithosphere noticed on seafloor curvature and marine complete Bouguer gravity anomalies across the Banda orogen. Seismic reflection data

from the northern Australian continental shelf-slope southwest of Timor Island (Fig. 1) show that the extent of normal faulting reduced significantly in Late Miocene–Early Pliocene (Fig. 2) (Lorenzo et al., 1998). Bending stress distribution, and the magnitude of bending moment depend on the value of EET and the curvature of the flexed lithosphere (Turcotte and Schubert, 1982). We attempt to establish a link between the changes in EET and decrease in normal faulting at the start of continental subduction in late Miocene–early Pliocene (Veevers et al., 1978; Johnston and Bowin, 1981) as seen on seismic reflection data (Fig. 2).

2. Geological background

The northern Australian continental lithosphere is in an incipient stage of continental collision across the Banda orogen where the continental crust on the shelf and slope is fairly uniform in thickness (Bowin et al., 1980). The depth of Moho of the northern Australian continental crust in the Timor Trough based on seismic refraction experiments is 29 km (Bowin et al., 1980). Using seismic refraction studies, thickness of the crust in the continental shelf near Australia is in the range of 31–35 km but thins to 26.6 km east of Aru Island (Bowin et al., 1980). The northern Australian continental lithosphere underwent NW striking rifting in Late Devonian–early Carboniferous (Petrel sub-basin in Fig. 1) and ENE-WSW striking Jurassic rifting (Malita graben in Fig. 1) (Gunn, 1988; Harris, 1991). The earliest record of collision between Australian and Eurasian lithosphere in Timor Island is marked by the presence of ~38 Ma (Late Eocene) metamorphic overprint on ophiolites (Sopaheluwaken et al., 1989). At DSDP 262 site in the Timor Trough (Fig. 1) the transition from shallow water to deep water sedimentation in the early Pliocene indicates that the subduction of northern Australian continental lithosphere started at least 3 Ma in the trough (Veevers et al., 1978; Johnston and Bowin, 1981).

Using He^3/He^4 and He^3/He^4–Sr^{87}/Sr^{86} isotope ratios from active volcanoes (Fig. 1), Hilton et al. (1992) detect northern Australian continental crust down to 100–150 km. In the northern Australian continental lithosphere, the shallower part of the lithosphere is believed to be in rebound (Chamalaun and Grady, 1978; Price and Audley-Charles, 1987; Charlton, 1991a). Earthquake foci north of the Banda orogen at intermediate depths (50–100 km) also suggest that the leading edge of the Australian lithosphere is presently detaching at those depths (McCaffrey et al., 1985; McCaffrey, 1988; Charlton, 1991a).

Evidence for continental collision across the entire Banda orogen is also found in the crustal shortening and thickening beneath the orogen manifested by the occurrence of high-angle shallow thrust earthquakes (McCaffrey and Abers, 1991) and the formation of Timor-Tanimbar-Aru Trough, Pliocene uplift documented in the orogen (Chappell and Veeh, 1978; De Smet et al. 1989) and active volcanism in Banda Arc (Fig. 1). The northern Australian continental lithosphere south of Roti near Ashmore Platform (Fig. 1) is now estimated to be converging with the Eurasian lithosphere (Warris, 1973) at a rate of 74 ± 2 mm/yr in a N 17°E ± 3° direction (DeMets et al., 1994) (Fig. 1). Eastward toward the Kai Plateau, the direction of convergence becomes almost sub-parallel or is at an acute angle to the Banda orogen with significant collision accommodated by strike-slip faulting (von der Borch, 1979; Harris, 1991; McCaffrey and Abers, 1991) (Fig. 1).

Collision west and east of Timor Island does strain partitioning differently compared to central Timor (Harris, 1991). By contrast, in central Timor, the advanced continental collision has absorbed the majority of the forearc basin (Savu Basin) (Simandjuntak and Barber, 1996) (Fig. 1). North of western and eastern part of Timor Island, the forearc basins still have considerable width and active volcanism in Banda Arc (Fig. 1). Subduction today is believed to have ceased in the Timor Trough (Snyder et al., 1996), especially adjacent to central part of Timor Island. The continental collision is now being accomodated by Alor and Wetar back-thrusting north of Timor Island (Snyder et al., 1996) (Fig. 1). Recent GPS calculations near Darwin (Australian Shelf) show that the northern Australian continental lithosphere–Eurasian lithosphere as one block is converging with regard to Sunda shelf at a 7% slower rate compared to DeMets et al.'s (1994) estimation but in the same direction (Genrich et al., 1996). Observations such as, lack of volcanism (Fig. 1) (Audley-Charles and Hooijer, 1973; Hamilton, 1974; Johnston and Bowin, 1981) and paucity of earthquakes at intermediate depths (Hamilton, 1974; Cardwell and Isacks, 1978) in the Banda Arc north of central Timor Island

also support this hypothesis (Genrich et al., 1996; Snyder et al., 1996).

The seismic reflection data on the northern Australian continental shelf-slope southwest of Timor Island (Fig. 1) show that the extent of normal faulting has changed through time (Fig. 2). The majority of extensional faulting which ends at Late Jurassic can be attributed to the cessation of the rifting (Gunn, 1988; Harris, 1991). Reactivation of older normal faults from Jurassic rifting in Eocene–Miocene (Fig. 2) could result from extensional stresses created during bending of the Australian lithosphere. This bending is due to the start of the subduction of the oceanic part of the Australian lithosphere in Late Eocene (Sopaheluwaken et al., 1989). Most of these normal faults cease to be active in Late Miocene–Early Pliocene (Fig. 2). However, there is evidence for present-day extensional faulting as seafloor scarps seen on the northern Australian continental slope but with a reduced areal extent on the continental shelf-slope (Boehme, 1996).

3. Surface and subsurface loading

To accurately estimate the EET of the northern Australian continental lithosphere, it is important to delineate the sources and magnitude of the geological loads (surface and subsurface) causing flexure. The northern Australian continental lithosphere is assumed to be bend under the weight of the Banda orogen (Fig. 3A) which acts as surface load (Royden and Karner, 1984).

In elastic half-beam modeling, a subsurface loading component is only invoked when surface loads alone cannot account for the deflection in the data. These subsurface loads could originate in the deeper parts of the lithosphere, as found in some other foreland basins e.g. Apennine foreland (Royden and Karner, 1984) (Fig. 3B). Slab pull could act as a hidden subsurface load bending the northern Australian continental lithosphere. On other hand, a complete detachment of the northern Australian continental lithosphere from the oceanic lithosphere would mean that there is no slab pull. However, a partial detachment or buoyancy of the continental lithosphere (Chamalaun and Grady, 1978; Price and Audley-Charles, 1987; Charlton, 1991a) would cause the effect of slab pull to be buffered (Fig. 3B). Slab pull could act as a hidden subsurface load bending the northern Australian continental lithosphere.

Other subsurface loads include ophiolites (Karner and Watts, 1983; Royden, 1993) and/or thrusting of dense mantle rocks (Abers and McCaffrey, 1994) (Fig. 3C). The presence of these hidden high-density loads can be estimated from a positive Bouguer anomaly (Karner and Watts, 1983) and/or presence of ophiolites (Sopaheluwaken et al., 1989) found within the Banda orogen. Assuming that the positive Bouguer gravity anomaly within the Banda orogen correspond to a high-density subsurface load (Fig. 3) (Karner and Watts, 1983), one can estimate its relative contribution to the loading of the foreland. Another possible cause of subsurface loading could be the corner flow (Stewart and Watts, 1997) evidenced by island arc volcanism north of the forearc basins, such as the Savu (Karig et al., 1987) and Weber basins (Milsom et al., 1996) (Fig. 3D).

4. Data

Modeled flexure is matched to ETOPO-5 bathymetry data which is gridded at 5 min (~9 km in the area of study) intervals (National Geophysical Data Center, 1988). Worldwide satellite-derived marine free-air gravity anomaly data (Sandwell and Smith, 1997) in the area across the Banda Arc is used to derive complete 3D Bouguer gravity anomalies. Sandwell and Smith's (1997) data is prepared from Geosat Geodetic Mission and ERS 1 Geodetic Phase with a horizontal resolution of ~10 km. The accuracy of the worldwide satellite-derived free-air gravity anomaly is 3–7 mGal (Sandwell and Smith, 1997). Marine complete 3D Bouguer gravity anomalies are created from the satellite-derived free-air gravity anomalies (Sandwell and Smith, 1997) by replacing the seawater by Tertiary sediments (Table 1) and applying 3D bathymetric corrections (Blakely, 1995; Tandon, 1998).

The seismic reflection section (Fig. 2) from Australian Geological Survey Organization (AGSO) traverses through Ashmore Platform shelf-slope region (Fig. 1) where northern Australian continental lithosphere believed to be in active continental-arc collision beneath the Timor Trough.

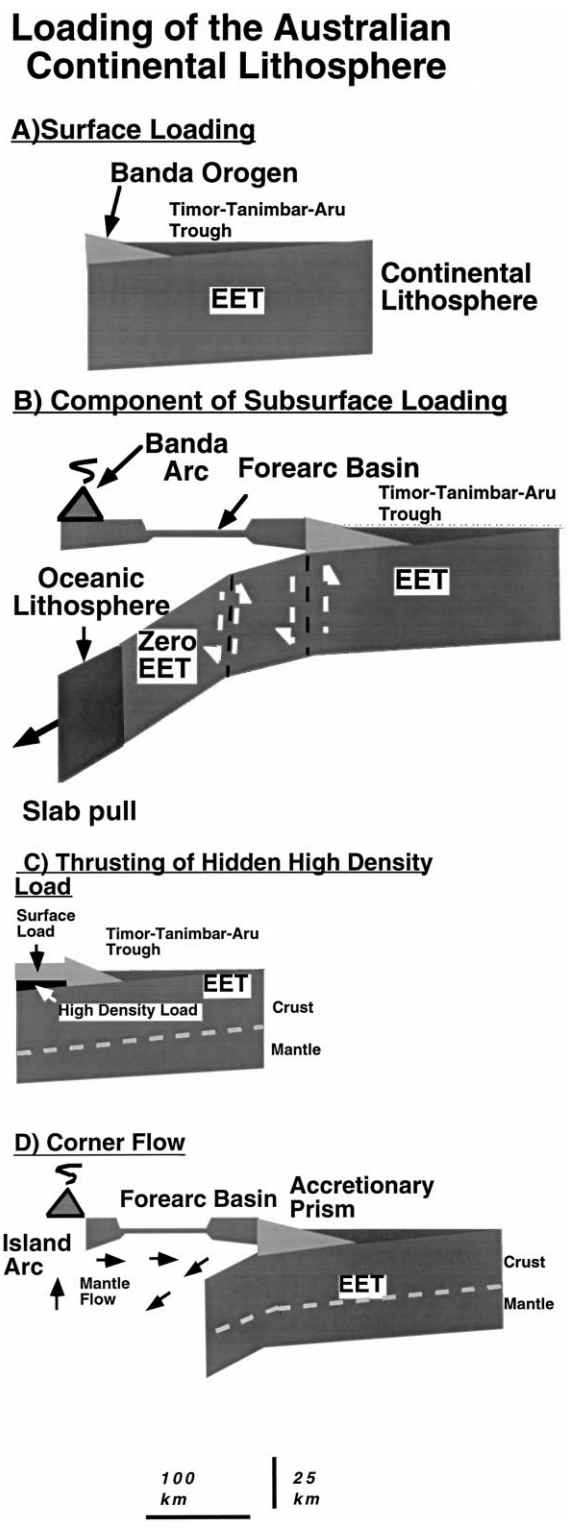
Loading of the Australian Continental Lithosphere
A)Surface Loading
Banda Orogen
Timor-Tanimbar-Aru Trough
EET
Continental Lithosphere
B) Component of Subsurface Loading
Banda Arc
Forearc Basin
Timor-Tanimbar-Aru Trough
Oceanic Lithosphere
EET
Zero EET
Slab pull
C) Thrusting of Hidden High Density Load
Surface Load
Timor-Tanimbar-Aru Trough
EET
High Density Load
Crust
Mantle
D) Corner Flow
Forearc Basin
Accretionary Prism
Island Arc
Mantle Flow
EET
Crust
Mantle
100 km
25 km

Table 1
Parameters (Chamalaun and Grady, 1976; Turcotte and Schubert, 1982; Richardson, 1999) used for (a) elastic half-beam, and (b) gravity modeling. All the units are defined in SI

Name	Value	Units
(a) **Elastic beam**		
Young's modulus (E)	1×10^{11}[a]	Pa
	5×10^{10}[b]	Pa
Poisson's ratio (γ)	0.25	
Timor–Tanimbar–Aru trough (sea water)		
Density	1035	kg/m^3
Supporting fluid (Mantle)		
Density	3300	kg/m^3
Triangular wedge (Banda orogen)		
Density	2670	kg/m^3
(b) **Gravity modeling density**		
Density		
Sea water	1030	kg/m^3
Tertiary sediments	2200	kg/m^3
Banda orogen	2670	kg/m^3
Australian continental crust	2800	kg/m^3
Mantle	3300	kg/m^3

[a] Used in the finite-difference formulation.
[b] Used in Heteyni's (1946) analytical approach.

Note: Our finite-difference scheme formulation (Bodine et al., 1981; Stewart and Watts, 1997; Lorenzo et al., 1998) uses Young's Modulus, $E = 1 \times 10^{11}$ Pa compared to 0.5×10^{11} Pa for Heteyni's (1946) analytical approach used for regional constant EET estimates. Given for the same amount of bending because of higher E, the estimates of constant EET from the finite-difference formulation are 20% lower (Turcotte and Schubert, 1982) compared to EET calculations from Heteyni's (1946) approach. We choose $E = 5 \times 10^{10}$ Pa for Heteyni's (1946) approach which is close to the values of $6–7 \times 10^{10}$ Pa used for continental lithosphere by Turcotte (1979). However, the compiled version of finite-difference scheme used by us had $E = 1 \times 10^{11}$ Pa for continental lithosphere.

5. Modeling

5.1. Basic assumptions and theory

We approximate the northern Australian continental lithosphere by an elastic half-beam model embedded in an inviscid fluid (Turcotte and Schubert, 1982) (Fig. 4). The northern Australian continental lithosphere has not been loaded long enough (from early Pliocene onwards $= \sim 5$ My) to warrant visco-elastic approximations (Beaumont, 1978; Turcotte, 1979; Beaumont, 1981). Walcott (1970) believes that visco-elastic behavior in a lithosphere operates from time scales ranging from 1 to 1000 Ma. However, Lorenzo et al. (1998) show that the absence of short-wavelength, high amplitude forebulge (caused by low EET values) on the continental shelf today is evidence for a presence for high EET values on northern Australian continental shelf. Maintaining high EET values on the continental shelf justifies

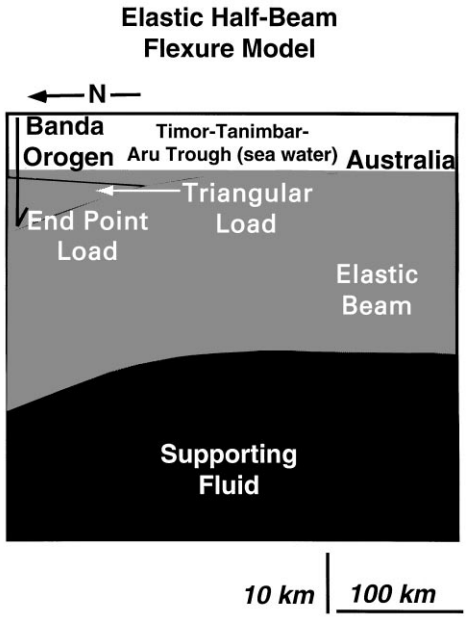

Fig. 4. An elastic half-beam model with uniform Effective Elastic Thickness (EET) is used to calculate the EET of the northern Australian continental lithosphere. The Banda orogen is approximated by a triangular load. The end-point load at the northern end of elastic half-beam approximates the subsurface component of loading (Fig. 3). Laterally variable EET model has the EET decreasing from Australia to Timor–Tanimbar–Aru trough to Banda orogen.

Fig. 3. Schematic description of the loading (Royden, 1993; Stewart and Watts, 1997) for the northern Australian continental lithosphere: (A) weight by the Banda orogen, (B) slab pull from a partially detached Australian lithosphere. Dip of the inferred detachment or partial detachment could be guessed from the earthquake foci by McCaffrey et al. (1985), McCaffrey (1988), and Charlton, (1991a). Slab pull is from the excess mass of the oceanic lithosphere (Forsyth and Uyeda, 1975), (C) hidden subsurface load (Karner and Watts, 1983), and (D) corner flow due to active arc magmatism (Royden, 1993; Stewart and Watts, 1997). EET is the measure of flexurally rigid part of the continental lithosphere incorporating crust and mantle.

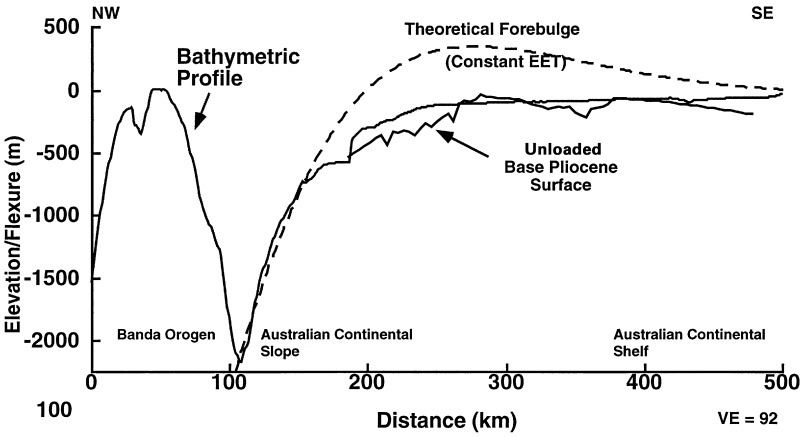

Fig. 5. Modeled flexure compared to the seafloor from ETOPO-5 (National Geophysical Data Center, 1988) and the unloaded base Pliocene surface (Boehme, 1996) southwest of Timor Island. Flexure computed by the elastic half-beam model with constant EET presented in Fig. 4 matches the slope but not the theoretical forebulge predicted on the continental shelf to seafloor bathymetry and base Pliocene surface. VE = Vertical Exaggeration.

elastic half-beam modeling. Elastic half-beam models have also been successfully applied in similar geological settings (Karner and Watts, 1983; Royden and Karner, 1984).

We use a half-beam model (Karner and Watts, 1983) (Fig. 4) instead of an infinite-beam model (Turcotte and Schubert, 1982) for elastic half-beam modeling. There is no evidence that the northern Australian continental subduction system and the forearc north of it acts as one rigid body which is being load by the Banda orogen. The shallower part of the northern Australian continental lithosphere is assumed to be in state of detachment based on field observations (Chamalaun and Grady, 1978; Price and Audley-Charles, 1987; Charlton, 1991a) and earthquake data (McCaffrey et al., 1985; McCaffrey, 1988) favoring a half-beam approximation.

A laterally variable EET model incorporates the decrease in EET due to inelastic processes, such as brittle and plastic failure, mechanical decoupling between upper-lower crust and mantle. A very subdued amplitude ($\leq$100 m amplitude with over hundreds of kilometer wavelength) of the forebulge on northern Australian continental lithosphere (Fig. 5) can be caused by inelastic/plastic failure on the continental slope to a high EET lithosphere on the northern Australian continental shelf (Lorenzo et al., 1998). Also, reactivation of faulting on the inherited rift-related structure at the continental shelf can further mask the observation of an idealized forebulge (Boehme, 1996; Lihou and Allen, 1996). High EET values ($\sim$50–80 km) create low amplitude, large wavelength forebulge on the continental shelf as opposed to low EET ($\sim$10–30 km) that form high amplitude, low wavelength forebulge for same amount of load. High EET values on the shelf with EET values decreasing down dip on the slope lower the amplitude of a forebulge further compared to a constant high EET estimate. Decreasing EET on the continental slope due to inelastic failure decreases the capacity of the continental lithosphere to transmit stresses and develop idealized forebulges (see Fig. 5) (McAdoo et al., 1978).

We estimate EET across an area southwest of Timor Island where an unloaded base Pliocene surface (the Plio-Quaternary sediments are removed) is available from seismic reflection data (Lorenzo et al., 1998) (Fig. 5). Both estimates for EET derived from modeling the unloaded base Pliocene surface (base foreland) and the seafloor are similar (Fig. 5) because the sedimentary cover from Recent-Pliocene is very thin (Boehme, 1996). The bottom of Pliocene surface on the northern Australian continental shelf is few hundred meters deep (Boehme, 1996). In the Timor Trough at DSDP 262 (Fig. 1), the depth to base Pliocene surface is $\sim$400 m (Veevers, 1974). The thickness at the trough is comparable to the thickness of Recent-Pliocene age sediments on the shelf. Due to limited availability of seismic reflection data

across the northern Australian continental lithosphere, we can not construct a regional uncompacted base Pliocene surface (base foreland) (Royden, 1988) for modeling flexure.

In our forward modeling for calculating EET, we use marine complete 3D Bouguer gravity anomalies (Fig. 6) instead of marine free-air anomalies (McKenzie and Fairhead, 1997). Marine complete Bouguer gravity anomalies remove the gravity effect of seafloor-water interface (Blakely, 1995; Tandon, 1998) enabling us to delineate intra-crustal heterogeneities and the Moho. The subduction of the flexed Moho at the outer trench slope and beneath the accretionary prism creates a negative Bouguer gravity anomaly of the order of 100 mGals spread over several hundred kilometers. We not only choose marine complete Bouguer anomalies to model elastic half-beam response to the subduction of flexed Moho but also use positive part of the Bouguer anomaly within the Banda orogen to identify high-density subsurface loads.

Small-wavelength gravity anomalies over the shelf of northern Australian continental lithosphere arise from the presence of horst and graben structures (Fig. 1) and igneous rocks related to the previous rifting (Anfiloff, 1988). Also, crustal heterogeneities at longer wavelengths and tectonic deformation other than continental subduction could mask the gravity signature of the flexed Moho. However, seismic refraction data (Bowin et al., 1980) show that the crustal structure on the northern Australian continental shelf and slope is quite homogeneous. We assume for our modeling that the change in dip angle in marine complete Bouguer gravity anomalies between different profiles are due to variation in EET. The changes in dip angle seen in marine Bouguer gravity anomalies over the continental slope have a wavelength of several hundreds of kilometer.

There will also be a long wavelength anomaly due to lithosphere–asthenosphere boundary in the subduction setting. However, upward continuation by hundreds of kilometers from the lithosphere–asthenosphere boundary will cause the effect to be spread over larger wavelength and smaller magnitude compared to the Bouguer gravity anomalies created by the crust mantle boundary.

5.2. Modeling seafloor

We use Hetenyi's (1946) analytical approach to solve the 2D flexure equation with parameters given in Table 1 for constant EET calculations (Chamalaun and Grady, 1978; Turcotte and Schubert, 1982; Richardson, 1999). In the elastic half-beam model, the flexure depression (Timor–Tanimbar–Aru Trough) is filled by seawater (Fig. 4). Also, in the elastic half-beam model, the Banda orogen is approximated by a triangular load with maximum height at its northern end (Fig. 4).

We attempt to match the seafloor to elastic half-beam modeling in a following fashion: (1) Match the predicted flexure to the northern Australian continental slope. (2) Minimize the modeled forebulge. Neither the unloaded base Pliocene sedimentary surface (Boehme, 1996; Lorenzo et al., 1998) nor the seafloor (National Geophysical Data Center, 1988) show a pronounced forebulge (Fig. 5). Therefore, boundary forces used should not accentuate the theoretical forebulge. (3) Match the maximum height of the triangular load on the flexed beam with the highest tip of the accretionary prism of the Banda orogen. (4) Determine the northern limit of the non-zero EET elastic half-beam by the total width of the triangular load that the elastic half-beam model can support. In our modeling effort, we initially attempt to match the width of the triangular load to the width of the Banda orogen loading a non-zero EET beam. The back-stop (start of profile in Fig. 5) is assumed to be the northern boundary for the accrectionary prism that separates it from the northern forearc basin (Fig. 1). This helps us estimate the width of the Banda orogen and acts as a starting northern limit for our elastic half-beam model. The width of the triangular load used in the model is a close approximation to the actual width of the Banda orogen (Harris, 1991; Richardson and Blundell, 1996). However, in some cases the width of the triangular load used on the elastic half-beam model is less than the observed width of the Banda orogen (Fig. 5). (5) We start our modeling with applying a triangular load and only use an end-point load at the northern end for elastic half-beam modeling if the triangular load is unable match the data (Fig. 4). The magnitude of the end-point load is determined by the best fitting model.

5.3. Laterally variable EET modeling

Laterally variable EET modeling for an elastic half-beam is done using a finite-difference scheme (Bodine et al., 1981; Stewart and Watts, 1997; Lorenzo et al.,

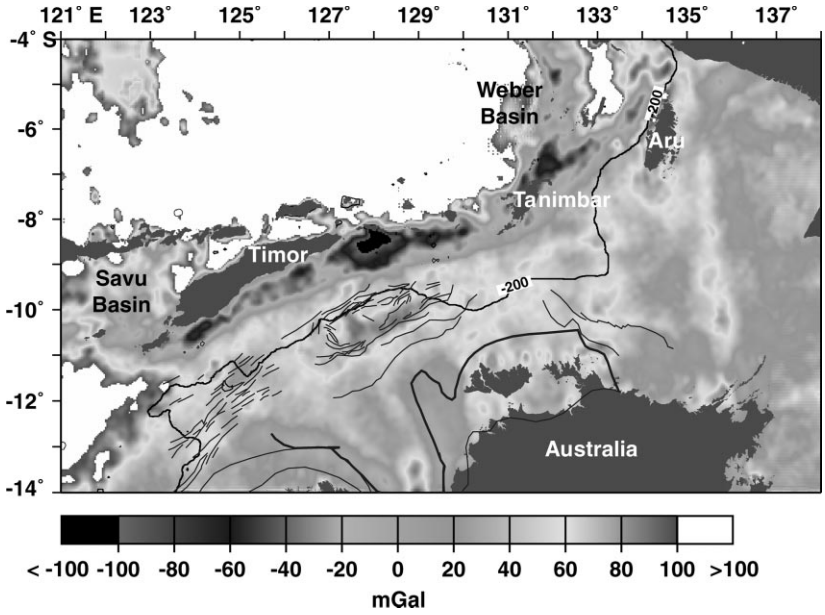

Fig. 6. Marine complete 3D Bouguer gravity anomalies for the northern Australian continental lithosphere across the Banda orogen. Dark grey area corresponds to the portion of the Banda arc above the sea level with no data coverage by the marine free-air gravity anomalies (Sandwell and Smith, 1997). Geological information overlain is from Fig. 1.

1998) to investigate the changes in the northern Australian continental lithosphere from the shelf to slope to beneath the orogen. A good match between the seafloor and the model (constant and laterally variable EET) is only considered if all the conditions described in last section are met. Laterally variable EET model with EET value decreasing down dip is able to also minimize the forebulge to a much greater degree than the constant EET model even when the EET values are similar on northern Australian continental shelf.

5.4. Modeling marine complete 3D Bouguer gravity anomalies

The theoretical Bouguer gravity anomalies for a flexed Moho are created from the density contrast given in Table 1. A theoretical Bouguer gravity anomaly created by a flexed Moho is then upward continued 29 km. The upward continuation of 29 km is equivalent to the depth of the Moho in northern Australian continental crust in the Timor Trough based on a seismic refraction experiment (Bowin et al., 1980). Similarly, theoretical Bouguer gravity anomalies assuming local area Airy isostasy (EET = 0 km) also use density values from Table 1 and are upward continued 29 km. Theoretical Bouguer gravity anomalies from a Moho in a local area isostasy shows us the deviation from local isostasy with respect to observed marine complete Bouguer gravity anomalies.

Assuming that the Moho is also flexed, Bouguer gravity anomalies derived from the best-matching elastic half-beam models using seafloor and a simple crustal model are matched to the profiles from the marine complete 3D Bouguer gravity anomalies. A good fit means that Bouguer gravity anomalies calculated from the elastic half-beam model match to the observed marine complete Bouguer gravity anomalies at the slope of the flexed lithosphere. Our fit for the gravity anomalies depends on the slope of the long wavelength negative Bouguer gravity anomaly due to subducted Moho.

The effect of prior rifting on a regional scale in northern Australian continental lithosphere is estimated using short-wavelength component of marine complete Bouguer gravity anomalies (Fig. 6). Structural information from seismic reflection data are only available for the sub-basins oriented ENE-WSW from Jurassic (Harris, 1991) and older NW striking rift basins from

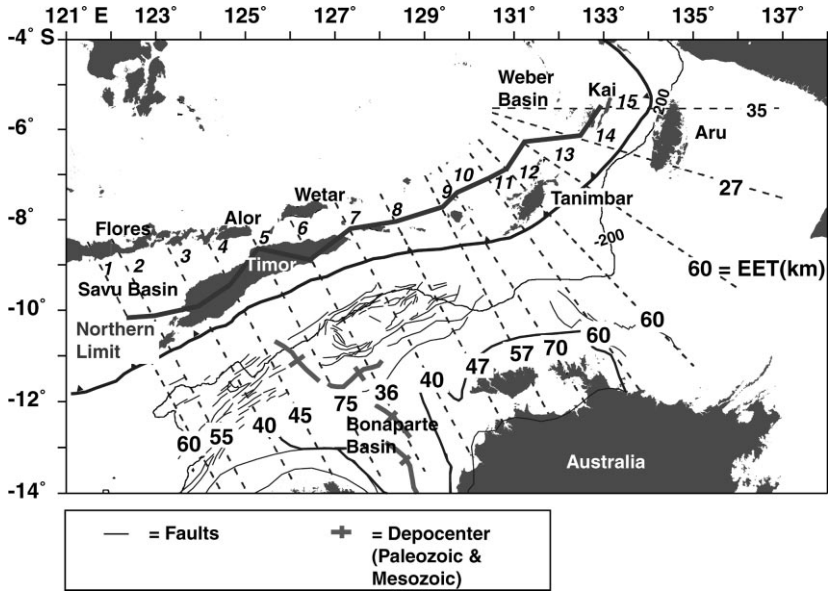

Fig. 7. Values of constant EET (km) for the northern Australian continental lithosphere across the Banda orogen. EET values are determined by bending of the elastic lithosphere via triangular loading and end-point loading (Fig. 4). The dashed lines locate transects used for the elastic half-beam modeling. The thick solid line lettered "northern limit", is the edge of the non-zero EET half-beam as determined by our model (Fig. 4). The details of the loading forces are given in Fig. 8.

Late Devonian–early Carboniferous (Gunn, 1988; Harris, 1991) (Petrel Sub-basin in Fig. 1) in the southwest corner of the study area (Stagg, 1993; AGSO North West Shelf Study Group, 1994). The marine complete Bouguer gravity anomaly map is only used to determine the distribution of the inherited structures on the northern Australian continental lithosphere where we do not have regional structural information (Fig. 6). Based on the regional structural geology map on the southwest (Fig. 1) and widespread occurrence of a similar patterns of small-wavelength Bouguer gravity anomalies caused by the horst-graben structure and rift volcanism (Anfiloff, 1988), it appears that past rifting affects the entire shelf of the northern Australian continental lithosphere in a similar fashion (Fig. 6). In a qualitative manner, we cannot differentiate the degree of rifting from one area to another in the northern Australian continental lithosphere based on data available to us (Fig. 6).

5.5. Uncertainty and sensitivity analyses

In general, given the uncertainties in the parameters used for elastic half-beam modeling (Table 1), the errors in the estimation of EET (Fig. 7) may be as high as 20% (Burov and Diament, 1995, 1996). We consider only EET variations $\geq$30% significant for testing the effect of different geological factors. A 30% error limit implies that an EET of 50 km could be in the range of 50 $\pm$ 15 km and yet get a reasonable match to the data without significantly altering the modeling parameters (Table 1). In one of our elastic half-beam modeling experiments, we use only an end-point load at the Timor–Tanimbar–Aru Trough in the elastic half-beam modeling, a variation of 0.2–0.4 $\times$ 10^{12} N/m^2 in end-point load changes the EET by 5–10 km and still matches the seafloor reasonably well. For EET = 35 km, a maximum 10 km variation in EET is close to the 30% error bound.

An order of magnitude decrease in the Young's Modulus (E) of the elastic half-beam results in increasing the EET by two-fold for same flexural rigidity. However, we keep most of the parameters fixed in our modeling (Table 1). For the same EET and load magnitude, a triangular load only produces a wider and shallower depression compared to applying

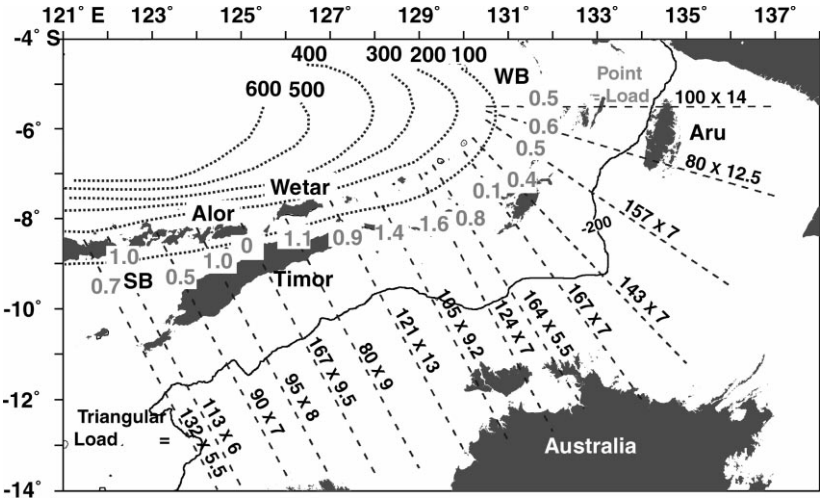

Fig. 8. Forces (surface and subsurface) loading the northern Australian continental lithosphere. These forces are used to compute the constant EET (km) in Fig. 7. The thick dashed lines are the 100 km contours for the Benioff seismic zone determined by earthquake locations (Hamilton, 1974). The triangular wedge used to approximate the Banda orogen is defined in terms of (1) length in km and (2) maximum width in km (shown on the northern Australian continental shelf). End-point loads are used for subsurface loading are to be multiplied by 10^{12} N/m^2 (shown near the Banda orogen). SB = Savu Basin and WB = Weber Basin.

an end-point load only. Therefore, applying triangular load requires higher values of EET to match the slope of northern Australian continental slope and marine complete Bouguer gravity anomalies.

On the eastern margin of the Banda orogen, the orocline can cause three-dimensional loading of the northern Australian continental lithosphere. A 2D formulation of flexure may result in an over-estimation of EET by 30% (Wessel, 1996) which is within the error bounds of our calculations. The effect of 3D could cause actual EET values to be lower than 2D estimations near Aru Island (Fig. 1).

6. Results

6.1. Constant EET values and seafloor

There is a wide range of EET (27–75 km) across the northern Australian continental lithosphere (Fig. 7). The highest value of EET (Profile 5 in Fig. 7) is present where the width of the forearc basin north of Timor Island is minimum and the continental collision along the Timor Trough has ceased today (Snyder et al., 1996; Genrich et al., 1996; Simandjuntak and Barber, 1996) (Fig. 1). However, the adjacent profile to the west (Profile 4 in Fig. 7) and to the east (Profile 6 in Fig. 7) has a lower value of EET where the collision is also believed to have ceased but the forearc basin north of Timor Island in those areas is still fairly wide (Fig. 1). Also, Profile 1 has higher value of EET than Profile 4 but the Savu basin is wider north of Profile 1 than Profile 4 (Fig. 7).

In Timor Island and the Kai Plateau, the width of the observed accretionary prism is greater than the width of the triangular load used for elastic half-beam modeling. In our modeling for these areas, the triangular load (Fig. 4) could not match the width of the entire accretionary prisms seen on the ETOPO-5 data and yet obey all our criteria used in the modeling. The "northern limit" in Fig. 7 shows where the elastic half-beam breaks beneath the Banda orogen. In general, end-point loads are an order of magnitude lower in the eastern part of the Banda orogen near the Kai Plateau (Fig. 8). No end-point load is needed for elastic half-beam modeling north of central Timor (Fig. 8).

6.2. Constant EET values and marine complete Bouguer anomalies

The theoretical Bouguer gravity anomalies derived

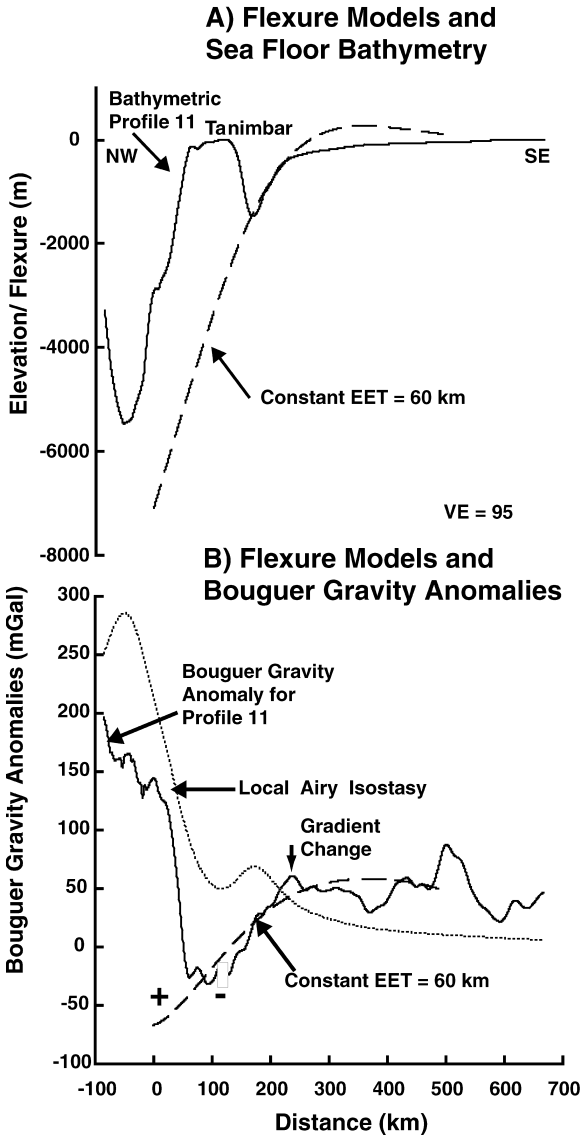

Fig. 9. EET values from profile 11 (Fig. 7) are determined by matching the flexural profile to the seafloor (National Geophysical Data Center, 1988). Theoretical Bouguer gravity anomalies created by a flexed Moho and assuming local area isostasy are then matched to the observed marine complete 3D Bouguer gravity anomalies. The origin of the profile is the northern limit of the non-zero EET elastic beam used along the transect (Fig. 7). ± = negative–positive Bouguer anomaly couple found traversing from the Banda orogen to the northern Australian continental slope. VE = Vertical Exaggeration. Notice that the gradient change in Bouguer gravity value does not correspond to shelf-slope boundary.

from constant EET calculations are in good agreement with the observed Bouguer gravity anomalies for profiles 1, 6, 7, 9, 11 (Fig. 9), 12 (Fig. 10), 13, and 14 (Tandon, 1998). The goodness of the match of theoretical Bouguer gravity anomalies to observed Bouguer gravity anomalies validates the EET calculations using seafloor independently for some of the profiles.

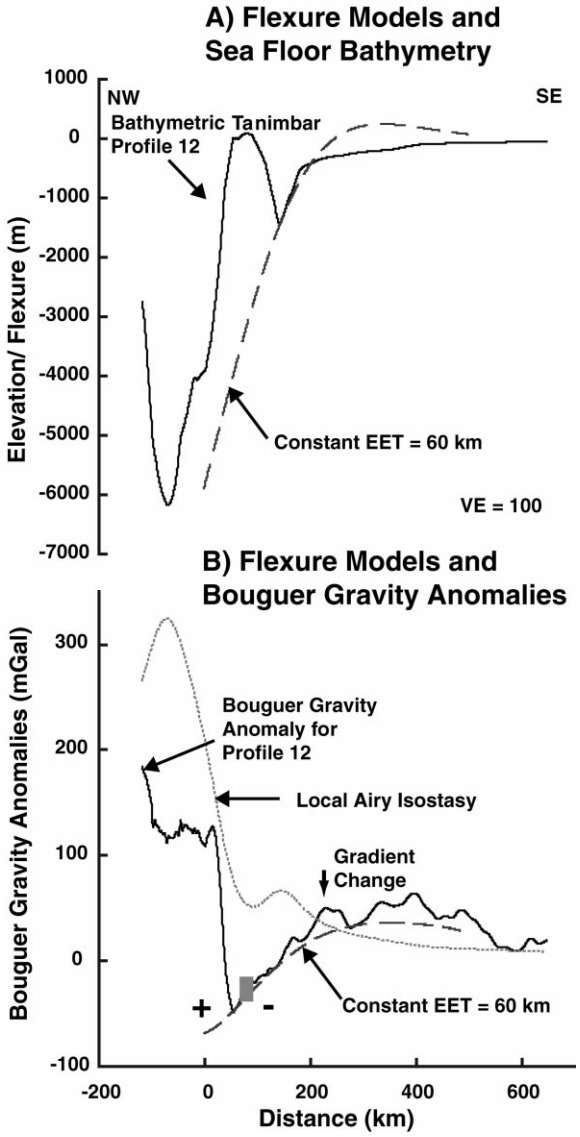

Fig. 10. EET values from profile 12 (Fig. 7). Similar explanation as in Fig. 9.

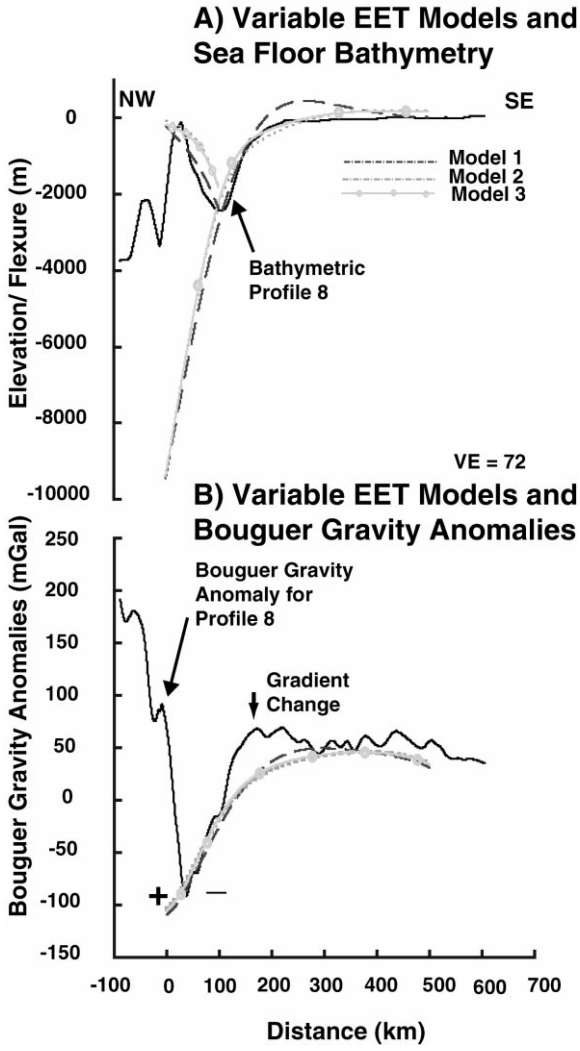

Fig. 11. Flexure and corresponding theoretical Bouguer gravity anomalies from elastic half-beam model using a laterally variable EET (km) across profile 8 (Fig. 7). The dimensions of the triangular load for laterally variable EET model is 9.2 km in maximum thickness at the edge and 105 km wide. The end-point load value is 0.8×10^{12} N/m^2. The northern limit of the elastic half-beam model for constant EET (Fig. 7) and laterally variable EET are the same. EET variations in Models 1 (constant EET), 2 (laterally variable EET), and 3 (laterally variable EET) from finite-difference method are explained in Fig. 12. Similar explanation as in Fig. 9.

However, along other profiles (2, 3, 4, 5, 8 (Fig. 11), 10, and 15), the slope of the theoretical Bouguer gravity anomalies derived from an elastic half-beam model does not match that well with the observed negative Bouguer gravity anomalies (Tandon, 1998). Fig. 11 clearly shows that shorter wavelength crustal heterogeneities (Anfiloff, 1988) do interfere with matching the theoretical Bouguer gravity response from an elastic half-beam model with only a simple crustal model to observed Bouguer gravity anomaly of subducting northern Australian continental lithosphere. Interestingly,

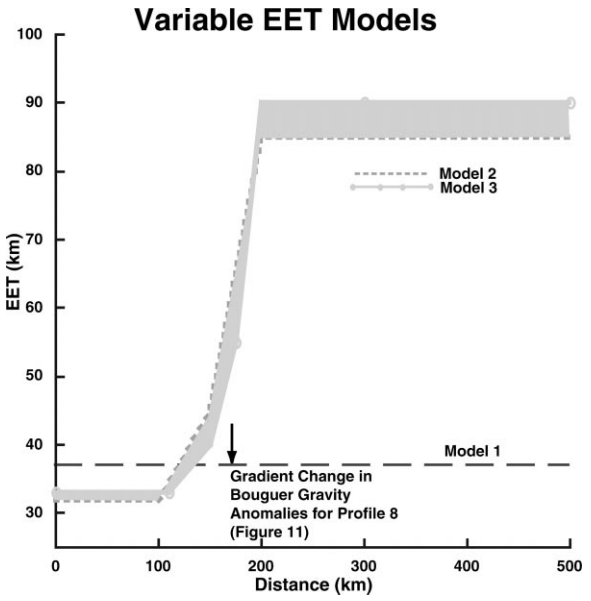

Fig. 12. Profile for variation in EET used for Fig. 11. The shaded area gives the range of possible values for EET fitting the seafloor using laterally variable EET model. The thick dashed line (Model 1) is the constant EET calculated using the finite-difference scheme. Models 2 and 3 constitute the upper and lower bounds of laterally variable EET which match the seafloor.

the observed Bouguer gravity anomalies and theoretical Bouguer anomalies for local Airy isostasy qualitatively match in regions north of non-zero EET region (Figs. 9–10).

6.3. Laterally variable EET profile

Laterally variable EET estimation shows that a change of ~90 to ~30 km is necessary to match the seafloor (Fig. 11A) and marine complete Bouguer gravity anomalies (Fig. 11B) along profile 8 (Fig. 7). Laterally variable EET modeling is able to match the seafloor better than a constant EET model by reducing the theoretical forebulge. The range of values in Fig. 12 shows the upper and lower limit of laterally variable EET (Models 2 and 3) where the flexure response fits the best on the northern Australian continental slope and the shelf. The shaded area between Models 2 and 3 are the acceptable values of EET using a laterally variable elastic half-beam model.

7. Discussion

7.1. Geological significance of an end-point load

The measured width of the positive Bouguer gravity anomaly on a non-zero EET beam does not correlate directly with the magnitude of the end-point load used for elastic half-beam modeling (Fig. 13). Width of a positive Bouguer gravity anomaly within the non-zero EET (Fig. 13) is attributed to hidden high-density load within the Banda orogen (Fig. 3). For example, in Profile 5 across central Timor (Fig. 7), the no end-point load used is needed even in a presence of positive Bouguer gravity anomaly (Fig. 13). We believe that the contribution of the high-density subsurface load which is clearly seen loading Australian continental lithosphere (Fig. 13) is being incorporated within the triangular load used in elastic half-beam model (Fig. 4). The high-density subsurface load created by ophiolites and dense mantle rocks is a part of the Banda orogen approximated by a triangular load. However, some part of high-density load is being taken up by end-point load.

The zero end-point load (Fig. 8) coincides with the area where the width of the forearc basin north of Timor Island is minimum and the continental collision along the Timor Trough has ceased today (Snyder et al., 1996; Genrich et al., 1996; Simandjuntak and Barber, 1996) (Fig. 1). We may assume that absence of slab pull by oceanic lithosphere might be linked to zero end-point load. It could be that highest EET values (Fig. 7) along with effect of the slab pull by the oceanic lithosphere almost removed promotes back-thrusting north of central Timor more than adjacent areas. However, hundreds of kilometers on either side, flexure profiles use end-point load of $1.0–1.1 \times 10^{12}$ N/m^2 (Fig. 8) with lower EET values compared to Profile 5 and there is back-thrusting north of Alor and Wetar (Fig. 1).

The northwest of Aru Island maybe experiencing a weakly buffered slab pull from oceanic lithosphere which is quantified by an end-point load equal to 0.6×10^{12} N/m^2. The link between end-point load and weakly buffered slab pull is speculative. Weakly buffered slab pull is invoked because northern Australian continental lithosphere is assumed to be detaching from the oceanic lithosphere (Chamalaun and Grady, 1978; Price and Audley-Charles, 1987;

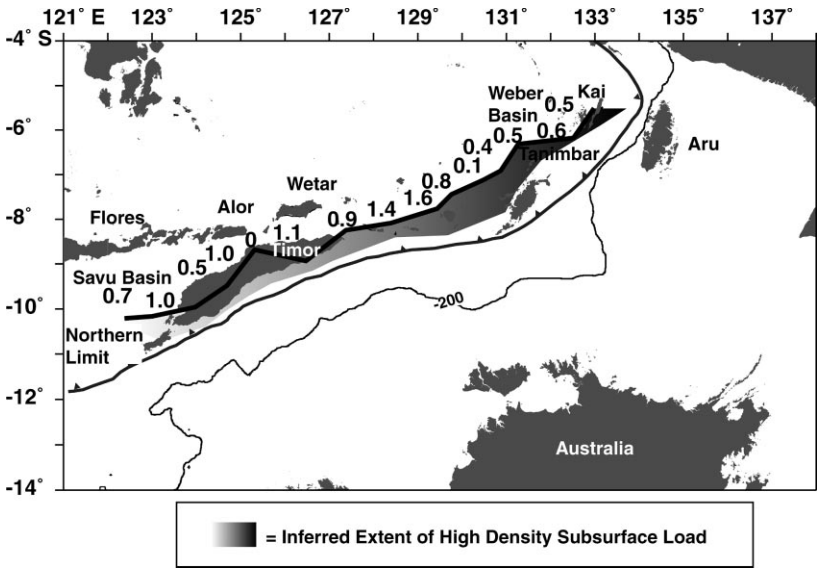

Fig. 13. Inferred width of the high-density subsurface loading does not compare to the magnitude of the end-point load ($\times 10^{12}$ N/m^2) used for elastic half-beam modeling. Other explanations similar to Fig. 7. This implies that the end-point could also be approximating other subsurface loading components (Fig. 13).

McCaffrey et al., 1985; McCaffrey, 1988; Charlton, 1991a). Also, the magnitude of point-load shows no link to the dip of the Benioff zone (Fig. 8) that would have otherwise implied a non-buffered slab pull. West of Aru Island, the presence of positive Bouguer gravity anomaly within the non-zero EET beam is almost non-existent (Fig. 13). Yet the end-point load used for the modeling is 0.6×10^{12} N/m^2 (Fig. 13). Absence of positive Bouguer anomaly within the non-zero EET beam northwest of Aru Island enables us to attempt a tentative quantification between the end-point load and weakly buffered slab pull. Establishing a link between subsurface loading in elastic half-beam modeling and higher resolution seismic tomography in future could help us resolve the contribution of slab pull in the formation of a continental foreland.

7.2. Geological Processes and variation of EET across the Banda orogen

There is a wide scatter in constant EET values from the 15 profiles (Fig. 7), which leads us to divide the northern Australian continental lithosphere into eight distinct EET provinces (Fig. 14). These changes in EET could be explained by inelastic failure within the elastic lithosphere.

A ~64% reduction is seen from EET values ranging from 75 to 27 km (Fig. 7). Such a reduction in EET assumes that at least ~75 km is a base value of constant EET for northern Australian lithosphere prior to reduction. A variation of 52% (profile 5 and 6 in Fig. 7) along with EET values from west of Timor to Tanimbar Island in constant EET calculations is perhaps due to variation in the amount of inelastic yielding across the northern Australian continental lithosphere. EET near Aru Islands is 41–55% lower than the EET in Tanimbar (Figs. 7 and 14) could be due to further inealstic yielding caused by the orocl-inal shape of northern Australian continental lithosphere in the region (Fig. 1). The radius of curvature in the eastern margin for the Australian lithosphere is calculated by matching an arc of the circle to the outline of the thrust sheets (McNutt et al., 1988) (Fig. 1). The log (radius of curvature) for the Banda orogen from Ceram to Tanimbar is ~2.5 km (Fig. 15). The EET values near Aru Trough are similar to estimates for EET in Western Alps, Carpathians, and Pamir, which have a similar radius of curvature (McNutt et al., 1988) (Fig. 15).

We expect constant EET values for the northern

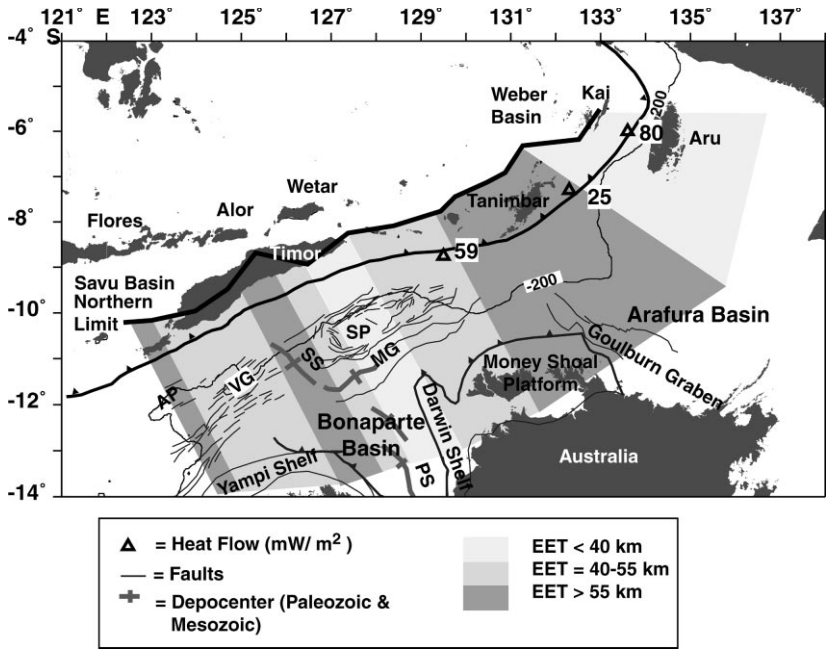

Fig. 14. Regions of similar EET (km) across the northern Australian continental lithosphere. Geological information is from Fig. 1. Other explanations similar to Fig. 7.

Australian continental lithosphere to be less than 30 km because less than ~200 My have elapsed between the last rifting (Harris, 1991) and the loading of the continental lithosphere (Watts, 1988, 1992; Stewart and Watts, 1997). Watts (1992) advocates that most continental foreland basins show a bi-modal distribution of either 10–20 or 80–90 km EET depending on the time duration between the last rifting and continental subduction. As the lithosphere gets thermally older, the stronger olivine rheology of the mantle dominates the strength of the lithosphere thereby increasing the EET (Kusznir and Karner, 1985). Alternately, rifting can also increase the EET of the lithosphere as the ratio of stronger mantle compared to weaker crust increases (Bertotti et al., 1997).

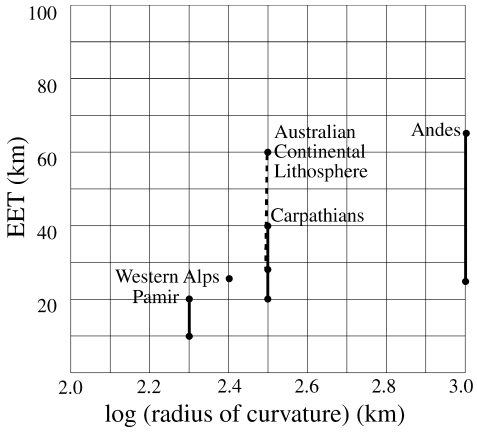

Fig. 15. Comparison of log (radius of curvature) (km) to the range of EET (km) values from the eastern margin of northern Australian continental lithosphere (from profile 11–15 in Fig. 7) to the values from western Alps, Andes, Carpathians, and Pamir (McNutt et al., 1988).

We do not find any link between the inferred rift architecture inferred from regional structural geology (Fig. 1) and marine complete Bouguer gravity anomalies (Fig. 6) to the distribution of EET (Fig. 14). Extension during the Jurassic rifting with ~20% strain observed on the outer NW Shelf of Australia (AGSO North West Shelf Study Group, 1994) indicates that the rifting had a limited effect on the EET of northern Australian continental lithosphere. Any effect on EET by a limited Jurassic rifting on the present-day continental shelf of northern Australian continental lithosphere could have now undergone thermal relaxation.

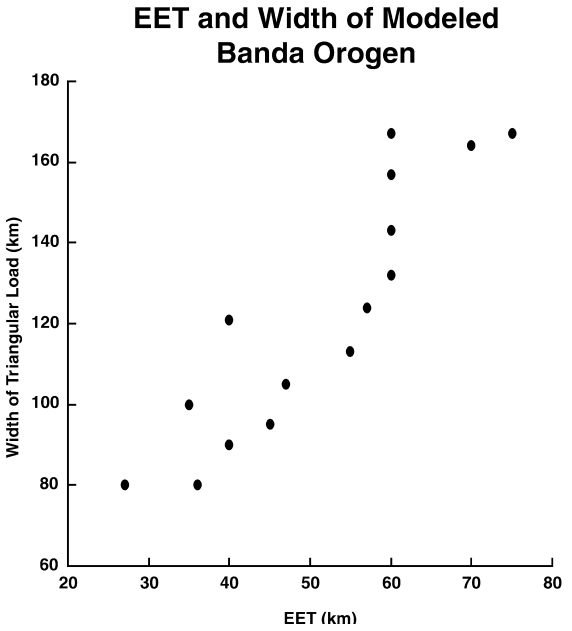

Fig. 16. Plot of computed EET (km) and the width of the triangular load (km) approximating the Banda orogen loading the non-zero EET part of the northern Australian continental lithosphere. The triangular load is an approximation for an accretionary prism in the elastic half-beam modeling. The plot shows the relationship between the EET and its effect on increased continental collision via the width of the accretionary prism.

7.3. Variation in EET and in continental collision tectonics

In Fig. 16, higher EET values correlate with a wider triangular load (Karig et al., 1976; Watts et al., 1995), which approximates the width of an accretionary prism while modeling. Central Timor is in its most advanced stage of collision across the Banda orogen (Harris, 1991) with the width of the island maximum (Fig. 1). Higher EET values make northern Australian lithosphere more resistant to bending. Combination of a higher EET Australian continental lithosphere aided by near-orthogonal convergence and slab detachment north of central Timor could have lead to more advanced collision. That is where the northern Australian continental lithosphere has the highest EET value (Figs. 7 and 14) and a widest triangular load (Fig. 8) compared to ones east and west of Timor Island. The variation between Profile 4 and 6 compared to Profile 5 (Fig. 7) is beyond the 30% error limit set for our modeling. Our modeled triangular load in central Timor has a width of 167 km and a maximum depth of 9.5 km (Fig. 8) which is quite similar to Charlton et al.'s (1991b) reconstruction.

Variations in EET and their link to the width of the triangular load in the northern Australian continental lithosphere (Fig. 16) can show how the distribution of EET could support the build-up of the wider accretionary prisms during continental subduction. Even at places where the northern Australian continental collision has not consumed almost all forearc basin north of Banda orogen (Figs. 7 and 14), the higher EET lithosphere leads to more thin-skinned tectonics compared to low EET lithosphere (Fig. 16). Highest EET values near central Timor (Figs. 7 and 14) agree rather well with the conclusions of Watts et al. (1995) from flexural modeling in central Andes.

Observation that parts of the width of the Banda orogen on Timor Island and in the Kai Plateau is not supported by the elastic half-beam model (Figs. 7 and 14) is also documented in flexure modeling for foreland adjacent to Himalayas (Lyon-Caen and Molnar, 1985) and in the New Guinea highlands (Abers and Lyon-Caen, 1990). Results from the northern boundary of the elastic half-beam model (Figs. 7 and 14) do not support the idea that the crustal thickening due to advancing continental collision decreases the EET beneath the orogen (Fig. 1). If so, then the northern Australian continental lithosphere near central Timor would not support the entire load of Timor Island in elastic half-beam modeling, contrary to the estimations as shown in Figs. 7 and 14.

7.4. Geological Processes and laterally variable EET from shelf to Banda orogen

The greatest lateral change in calculated EET values (Fig. 12) occurs at continental shelf-slope at normal crustal thickness (Bowin et al., 1980) and not beneath the Banda orogen. The bending stresses causing inelastic failure (Turcotte and Schubert, 1982) and EET reduction are maximum (~66% with respect to 90 km in Fig. 12) at the continental slope. Such a significant reduction in EET laterally cannot be delineated in constant EET estimates that has a bias toward matching the slope of the data.

Therefore, a laterally variable EET model documents that matching the curvature of the data is a more accurate way of estimating EET of a lithosphere.

7.5. Reduction of EET at the start of continental subduction

Prior to continental subduction, a very high EET lithosphere (at least ~75 km) created a large areal extent and also a larger magnitude of bending stresses that might have caused the Eocene–Miocene reactivation of Jurassic faulting on the present-day northern Australian continental shelf-slope (Fig. 2). These normal faults could cease to be active in late Miocene–early Pliocene because either the EET or the curvature of the northern Australian lithosphere in cross-sectional view reduced. Bending stresses depend on the EET and the curvature of the elastic lithosphere (Turcotte and Schubert, 1982).

Reduction in EET due to inelastic yielding at late Miocene–early Pliocene could be the cause for reduction in areal extent of normal faulting on the northern Australian continental shelf-slope (Fig. 2). Subduction of northern Australian continental lithosphere beneath the Banda orogen in late Miocene–early Pliocene (Veevers et al., 1978; Johnston and Bowin, 1981) will increase the curvature of the elastic lithosphere through time at any given point seaward of the forebulge.

Reduction in bending stresses can explain a decrease in extent of normal faulting but not cessation of normal faulting mostly seen on present-day continental shelf in Late Miocene–Early Pliocene (Fig. 2). Regional mapping on the shelf-slope shows that there is reduction in the areal extent of normal faulting on the present-day northern Australian continental shelf-slope compared to Early Pliocene (Boehme, 1996). Ideally, the present-day continental shelf-slope on the Ashmore Platform (Fig. 1) shown by the seismic reflection section (Fig. 2) should be under extension today due to the bending of northern Australian continental lithosphere.

There is a possibility that the reduced bending stresses due to decrease in EET are being almost neutralized by an overprint of increased regional compressive stress created by northern Australian-Banda Arc collision. This combination can cause the cessation of normal faulting in Late Miocene-Early Pliocene in parts of present-day northern Australian continental shelf (Karner, pers. commun.). A decrease in faulting due to inelastic failure at the start of northern Australian continental subduction assumes a simple lithospheric rheology, which does not include time-varying effect on lithospheric strength. However, the cessation of normal faulting near late Miocene–early Pliocene seems instantaneous on the seismic reflection data (Fig. 2).

7.6. Effect of other processes on EET

Three available single heat flow measurements (Fig. 1) do not provide a detailed insight to the thermal regime to northern Australian continental lithosphere. However, they enable us to do a cursory link between the heat flow and the EET calculations. Heat flow values vary by a factor of more than three from 25 to 80 mW/m^2 in the Banda Sea region (Bowin et al., 1980) (Fig. 1). This variation by a factor of two in the heat flow does not correlate with the calculated EET values of the northern Australian continental lithosphere within the error limits set for this study (Fig. 14).

8. Conclusions

Our constant EET estimations range from 27 to 75 km across the northern Australian continental lithosphere with highest value is in the vicinity of central Timor. In that area the continental collision is most advanced, the width of the island is maximum and the forearc basin north of Timor island is almost destroyed. From the shelf to the slope of northern Australian continental lithosphere, the reduction in EET in a laterally variable EET model is 66% (~90 km on shelf to ~30 km beneath the Banda orogen). The maximum decrease in EET is noticed on shelf-slope where the bending stresses are maximum. Variations in EET are linked to inelastic yielding in the northern Australian continental lithosphere at the beginning of continental subduction (late Miocene–early Pliocene). Seismic reflection data on the continental shelf-slope southwest of Timor Island supports the hypothesis of reduction in EET at the start of continental subduction. Variation in EET from west of Timor Island to Tanimbar could be manifested by varying degree of inelastic failure. Oroclinal bending of the northern Australian continental lithosphere

toward east (from Tanimbar to Kai Plateau) is causing further decrease in EET.

Wider triangular loads loaded by high EET show a link between EET and thin-skinned collisional tectonics creating broader accretionary prisms, destruction of forearc basins, and back-thrusting. Lack of end-point load beneath central Timor Island may indicate there is no slab pull from the leading edge of Australian lithosphere there.

Acknowledgements

This research was supported by graduate assistantships for KT from the Department of Geology and Geophysics, and Coastal Studies Institute, Louisiana State University (LSU) and research grant to JML from Petroleum Research Fund, administered by the American Chemical Society. Finite-difference code used for laterally variable EET modeling was kindly given to us by Jonathan Stewart (code originally written by Bodine). Some of the figures are made using the GMT software (Wessel and Smith, 1995). We thank Ricky Boehme, P.J. Perry, Giovanni Sella, Uwe Strecker and the dissertation committee at LSU for helping in improving earlier versions of the manuscript. General discussion on various aspects of flexure with Garry Karner was very beneficial to KT. We acknowledge the computer facilities provided by Julitta Kirkova, Chuck Payne, Dmitry Bazykin, and Sands Weems IV to KT for the preparation of this manuscript. The authors are grateful to David Wight from Geotools, AOA Geophysics Inc. for support to KT during final submission of this manuscript. Detailed Tectonophysics reviews by Suerke Planke, two anonymous reviewers, and the Guest Editor Montserrat Torne greatly improved the quality of the manuscript. The enclosed research was a part of dissertation work conducted by KT at Louisiana State University.

References

Abers, G.A., Lyon-Caen, H., 1990. Regional gravity anomalies, depth of the foreland basin and isostatic compensation of the New Guinea highlands. Tectonics 9, 1479–1493.

Abers, G.A., McCaffrey, R., 1994. Active arc-continent collision: earthquakes, gravity anomalies, and fault kinematics in the Huon–Finisterre collision zone, Papua New Guinea. Tectonics 13, 227–245.

AGSO North West Shelf Study Group, 1994. Deep reflections on the north west shelf: changing perceptions of basin formation. In: Purcell P.G., Purcell R.R. (Eds.), The North West Shelf, Australia. Proceedings of Petroleum Exploration Society of Australia symposium, pp. 63–76.

Anfiloff, V., 1988. Polycyclic rifting — an interpretation of gravity and magnetics in the North West Shelf. In: Purcell, P.G., Purcell, R.R. (Eds.), The North West Shelf, Australia: proceedings of petroleum exploration society of Australia symposium, pp. 443–455.

Audley-Charles, M.G., Hooijer, D.A., 1973. Relation of Pleistocene migrations of pygmy stegodonts to Island arc tectonics in eastern Indonesia. Nature 241, 197–198.

Beaumont, C., 1978. The evolution of sedimentary basins on a viscoelastic lithosphere: theory and examples. Geophys. J. R. Astron. Soc. 55, 471–497.

Beaumont, C., 1981. Foreland basins. Geophys. J. R. Astron. Soc. 65, 291–329.

Bertotti, G., ter Voorde, M., Cloetingh, S., Picotti, V., 1997. Thermomechanical evolution of the South-Alpine rifted margin (north Italy): Constraints on the strength of passive continental margins. Earth Planet. Sci. Lett. 146, 181–193.

Blakely, R.J., 1995. Potential Theory in Gravity and Magnetic Applications. Cambridge University Press, New York.

Bodine, J.H., Steckler, S.M., Watts, A.B., 1981. Observations of flexure and rheology of the oceanic lithosphere. J. Geophys. Res. 86, 3695–3707.

Boehme, R.S., 1996. Stratigraphic response to Neogene tectonism on the Australian Northwest Shelf. MS thesis, Louisiana State University, Baton Rouge, USA.

von der Borch, C.C., 1979. Continent-island arc collision in the Banda arc. Tectonophysics 54, 169–193.

Bowin, C., Purdy, G.M., Johnston, C., Shor, G., Lawver, L., Hartono, H.M.S., Jezek, P., 1980. Arc-continent collision in Banda Sea region. Am. Assoc. Petrol. Geol. Bull. 64, 868–915.

Burov, E.B., Diament, M., 1995. The effective elastic thickness (EET) of continental lithosphere: What does it really mean?. J. Geophys. Res. 100, 3905–3927.

Burov, E., Diament, M., 1996. Isostasy, equivalent elastic thickness, and inelastic rheology of continents and oceans. Geology 24, 419–422.

Cardwell, R.K., Isacks, B.L., 1978. Geometry of the subducted lithosphere beneath the Banda Sea in eastern Indonesia from seismicity and fault plane solutions. J. Geophys. Res. 83, 2825–2838.

Chamalaun, F.H., Grady, A.E., 1978. The tectonic development of Timor: a new model and its implications for petroleum exploration. Aust. Petrol. Explor. Assoc., 102–108.

Chappell, J., Veeh, H.H., 1978. Late quaternary tectonic movements and sea-level changes at Timor and Atauro Island. Geol. Soc. Am. Bull. 89, 356–368.

Charlton, T.R., 1991a. Post collision extension in arc-continent collision zone, eastern Indonesia. Geology 19, 28–31.

Charlton, T.R., Barber, A.J., Barkham, S.T., 1991b. The structural evolution of the Timor collision complex, eastern Indonesia. J. Struct. Geol. 13, 489–500.

DeMets, C., Gordon, R.G., Argus, D.F., Stein, S., 1994. Effects of recent revisions to the geomagnetic reversal time scale on estimates of current plate motions. Geophys. Res. Lett. 21, 2191–2194.

De Smet, M.E.M., Fortuin, A.R., Troelstra, S.R., Van Marle, L.J., Karmini, M., Tjokrospoetro, S., Hadiwasastra, S., 1990. Detection of collision-related vertical movements in the outer Banda arc (Timor, Indonesia), using micropaleontological data. J. Southeast Asian Earth Sci. 4, 337–356.

Dresen, G., Duyster, J., Stockhert, B., Wirth, R., Zulauf, G., 1997. Quartz dislocation microstructure between 7000 m and 9100 m depth from the Continental Drilling Program KTB. J. Geophys. Res. 102, 18 443–18 452.

Forsyth, D., Uyeda, S., 1975. On the relative importance of the driving forces of plate motion. Geophys. J. R. Astron. Soc. 65, 163–200.

Genrich, J.F., Bock, Y., McCaffrey, R., Calais, E., Stevens, C.W., Subarya, C., 1996. Accretion of the southern Banda arc to the Australian plate margin determined by global positioning system measurements. Tectonics 15, 288–295.

Gunn, P.J., 1988. Bonaparte rift basin: effects of axial doming and crustal spreading. Explor. Geophys. 19, 83–87.

Hamilton, W., 1974. Tectonics of the Indonesian region, US Govt. Printing Office, 1974.

Harris, R.A., 1991. Temporal distribution of strain in the active Banda orogen: a reconciliation of rival hypotheses. J. Southeast Asian Earth Sci. 6, 373–386.

Hetenyi, M.I., 1946. Beams on Elastic Foundation: Theory with Applications in the Field of Civil and Mechanical Engineering. The University of Michigan Press, Ann Arbor.

Hilton, D.R., Hoogewerff, J.A., van Bergen, M.J., Hammerschmidt, K., 1992. Mapping magma sources in the east Sunda-Banda arcs, Indonesia: constraints from helium isotopes. Geochim. Cosmochim. Acta 56, 851–859.

Johnston, C.R., Bowin, C.O., 1981. Crustal reactions resulting from the Mid-Pliocene to Recent continent-island arc collision in the Timor region. Aust. Bur. Miner. Resour. Geol. Geophys. J. 6, 223–243.

Karig, D.E., Caldwell, J.G., Parmentier, E.M., 1976. Effects of accretion on the geometry of the descending lithosphere. J. Geophys. Res. 81, 6281–6291.

Karig, D.E., Barber, A.J., Charlton, T.R., Klemperer, S., Hussong, D.H., 1987. Nature and distribution of deformation across the Banda arc-Australian collision zone at Timor. Geol. Soc. Am. Bull. 98, 18–32.

Karner, G.D., Watts, A.B., 1983. Gravity anomalies and flexure of the lithosphere at mountain ranges. J. Geophys. Res. 88, 10 449–10 477.

Kusznir, N., Karner, G., 1985. Dependence of the flexural rigidity of the continental lithosphere on rheology and temperature. Nature 316, 138–142.

Lavier, L.L., Steckler, M.S., 1997. The effect of sedimentary cover on the flexural strength of continental lithosphere. Nature 389, 476–479.

Lihou, J.C., Allen, P.A., 1996. Importance of inherited rift margin structures in the early North Alpine foreland basin, Switzerland. Basin Res. 8, 425–442.

Lorenzo, J.M., O'Brien, G.W., Stewart, J., Tandon, K., 1998. Inelastic yielding and forebulge shape across a modern foreland basin: north west shelf of Australia, Timor Sea. Geophys. Res. Lett. 9, 1455–1458.

Lyon-Caen, H., Molnar, P., 1985. Gravity anomalies, flexure of the Indian Plate and the structure, support and evolution of the Himalaya and Ganga basin. Tectonics 4, 513–538.

McAdoo, D.C., Caldwell, J.G., Turcotte, D.L., 1978. On the elastic-perfectly plastic bending of the lithosphere under generalized loading with application to the Kuril Trench. Geophys. J. R. Astron. Soc. 54, 11–26.

McCaffrey, R., 1988. Active tectonics of the eastern Sunda and Banda arcs. J. Geophys. Res. 93, 15 163–15 182.

McCaffrey, R., Abers, G.A., 1991. Orogeny in arc-continent collision: The Banda arc and western New Guinea. Geology 19, 563–566.

McCaffrey, R., Molnar, P., Roeker, S.W., Joyodiwiryo, Y.S., 1985. Microearthquake seismicity and fault plane solutions related to arc-continent collision in the eastern Sunda arc, Indonesia. J. Geophys. Res. 90, 4511–4528.

McKenzie, D., Fairhead, D., 1997. Estimates of the effective elastic thickness of the continental lithosphere from Bouguer and free air gravity anomalies. J. Geophys. Res. 102, 27 523–27 552.

McNutt, M.K., Diament, M., Kogan, M.G., 1988. Variations of elastic plate thickness at continental thrust belts. J. Geophys. Res. 93, 8825–8838.

Milsom, J., Kaye, S., Sardjono, 1996. Extension, collision, and curvature in the eastern Banda arc. In: Hall, R., Blundell, D. (Eds.), Tectonic Evolution of Southeast Asia. Geol. Soc. Sp. Publ. 106, 85–94.

National Geophysical Data Center, ETOPO-5 bathymetry/topography data, National Oceanic and Atmospheric Administration, US Dept. Commerce, Boulder, CO, 1988.

Price, N.J., Audley-Charles, M.G., 1987. Tectonic collision processes after plate rupture. Tectonophysics 140, 121–129.

Richardson, A., 1999. Constraints on continent-arc collision in eastern Indonesia, (preprint).

Richardson, A.N., Blundell, D.J., 1996. Continental collision in the Banda arc. In: Hall, R., Blundell, D. (Eds.), Tectonic evolution of southeast Asia. Geol. Soc. Sp. Publ. 106, 47–60.

Royden, L., Karner, G.D., 1984. Flexure of the continental lithosphere beneath Apennine and Carpathian foredeep basins. Nature 309, 142–144.

Royden, L., 1988. Flexural behavior of the continental lithosphere in Italy: constraints imposed by gravity and deflection data. J. Geophys. Res. 93, 7747–7766.

Royden, L., 1993. The tectonic expression slab pull at continental convergent boundaries. Tectonics 12, 303–325.

Sandwell, D.T., Smith, W.H.F., 1997. Marine gravity anomaly from Geosat and ERS 1 satellite altimetry. J. Geophys. Res. 102, 10 039–10 054.

Simandjuntak, T.O., Barber, A.J., 1996. Contrasting tectonics styles in the Neogene orogenic belts of Indonesia. In: Hall, R., Blundell, D., Tectonic evolution of southeast Asia. Geological Society Special Publication 106, 185–201.

Snyder, D.B., Prasetyo, H., Blundell, D.J., Pigram, C.J., Barber,

A.J., Richardson, A., Tjokosaproetro, S., 1996. A dual doubly vergent orogen in the Banda arc continent-arc collision zone as observed on deep seismic reflection profiles. Tectonics 15, 34–53.

Sopaheluwakan, J., Helmers, H., Tjokrosapoetro, S., Surya Nila, E., 1989. Medium pressure metamorphism with inverted thermal gradient associated with ophiolite nappe emplacement. Netherlands Journal of Sea Research, 24, 333–343.

Stagg, H.M.J., 1993. Tectonic elements of the north west shelf, Australia, scale 1:2500000, Australian Geological Survey Organization, Canberra.

Steckler, M.S., ten Brink, U.S., 1986. Lithospheric strength variations as a control on new plate boundaries: examples from the northern Red Sea region. Earth Planet. Sci. Lett. 79, 120–132.

Stewart, J., Watts, A.B., 1997. Gravity anomalies and spatial variation of flexural rigidity at mountain ranges. J. Geophys. Res. 102, 5327–5352.

Tandon, K., 1998. A Study of Models and Controls for Basin Formation During Continental Collision: (1) Australian Lithosphere along Banda Orogen (Indonesia) and (2) Alboran Sea Basin (Western Mediterranean), PhD dissertation, Louisiana State University, Baton Rouge, USA.

Turcotte, D.L., 1979. Flexure. Adv. Geophys. 21, 51–85.

Turcotte, D.L., Schubert, G., 1982. Geodynamics: Application of Continuum Physics to Geological Problems. Wiley, New York.

Veevers, J.J., Heirtzler, J.R. et al., 1974a. Initial reports of the Deep Sea Drilling Project, 27, 1060 pp.

Veevers, J.J., 1974b. Sedimentary sequences of the Timor Trough, Timor, and the Sahul shelf. In: J.J. Veevers, J.R. Heirtzler, et al. (Eds.), Initial Reports of the Deep Sea Drilling Project. vol. 27, pp. 567–569.

Veevers, J.J., Falvey, D.A., Robins, S., 1978. Tectonophysics 45, 217–227.

Walcott, R.I., 1970. Flexural rigidity thickness and viscosity of the lithosphere. J. Geophys. Res. 75, 3268–3941.

Warris, B.J., 1973. Plate tectonics and the evolution of the Timor Sea, northwest Australia. The Australian Petroleum Exploration Association, pp. 13–18.

Watts, A.B., 1983. The strength of the earth's crust. Mar. Technol. Soc. J. 17, 5–17.

Watts, A.B., 1988. Gravity anomalies, crustal structure and flexure of the lithosphere at the Baltimore canyon Trough. Earth Planet. Sci. Lett. 89, 221–238.

Watts, A.B., 1992. The effective elastic thickness of the lithosphere and the evolution of foreland basins. Basin Res. 4, 169–178.

Watts, A.B., Lamb, S.H., Fairhead, J.D., Dewey, J.F., 1995. Lithospheric flexure and bending of the central Andes. Earth Planet. Sci. Lett. 134, 9–21.

Wessel, P., Smith, W.H.F., 1995. New version of generic mapping tools. Eos Trans. AGU Electron. Suppl. (http://www.agu.org/eos-elec/95154e.html).

Wessel, P., 1996. Analytical Solutions for 3D flexural deformation semi-infinite elastic plates. Geophys. J. Int. 124, 907–918.